N84 27305

VARIATIONS IN SURFACE CURRENT OFF THE COASTS OF CANADA AS INFERRED FROM INFRARED SATELLITE IMAGERY

W.J. Emery, M. Ikeda, L.A. Mysak and P.H. LeBlond
Department of Oceanography
University of British Columbia
Vancouver, B.C. V6T 1W5, Canada

ABSTRACT

Infrared satellite images of sea surface temperature are used to infer changes in the surface currents off both the east and west coasts of Canada. Off the east coast summer infrared temperature patterns suggest a close connection between the location of the continental slope and the path of the Labrador Current as marked by a strong thermal front. Meanders and eddies appear to form where abrupt changes in the shape of the continental slope occur. In winter both infrared and visible imagery reveal the southward propagation of wavelike features in the ice patterns along the Labrador coast. A relatively large number of images from the Canadian west coast have been used to depict the evolution of surface temperature features associated with fluctuations in the corresponding current system. In winter and spring 150 km current meanders are fed energy by the baroclinic instability of the uniformly directed current which flows northwest in winter and southeast in spring. In summer the surface current is directed southeastward while below it an undercurrent flows to the northeast. Initiated by an interaction with the irregularities of the local continental slope 75 km current meanders begin to form. Energy is then fed non-linearly by baroclinic instability into longer scale 150 km meanders which eventually shed to form separate eddies.

INTRODUCTION

Infrared satellite imagery have often been used in oceanography to suggest the complexities of the ocean and to infer characteristics of surface currents possibly connected to the sea surface temperature patterns. By using a sequence or collection of such images it should be possible to examine both spatial and temporal changes in the infrared thermal patterns in an effort to better describe and understand the oceanographic mechanisms associated with these observed changes. In such a study it must be realized that while infrared satellite imagery has the limitation that it can only sense at the sea surface it also has the significant advantage that it can view a large part of the ocean in a truely synoptic fashion. Thus is provides oceanographers with a unique view of the ocean and studies using these images should focus on this advantage by looking for space and time scales clearly represented in the thermal imagery. In this way satellite infrared imagery can provide meaningful insight into ocean dynamics without the stringent requirements of providing precise and accurate surface temperature measurements.

Unfortunately for this study only a very limited number of digital images were available for the Canadian east coast which restricts the type of study that can be carried out. We will therefore only look at a few examples of summer imagery that suggest some interesting relationships between surface temperature patterns and details in the coastal bottom topography. Winter ice patterns will also be examined which suggest the southward, along-coast propagation of wavelike features at the edge of the ice. An earlier study by LeBlond (1982) identified these features in a sequence of four visible satellite images. From changes in the patterns of the ice edge he inferred a southeastward phase speed of features with a 73 km wavelength. Similar features are evident in some of the 18 winter/spring images examined in this study.

A substantially larger number of images was used to study changes in infrared surface temperature patterns off the Canadian west coast. Starting in the spring of 1980 arrangements were made to receive digital AVHRR data from a receiving station in Edmonton, Alberta operated by the Canadian Atmospheric Environment Service (AES). Most of the AVHRR images discussed in this study are recorded at this facility. Recently, however, a receiving station has been set up and is operating at the Department of Oceanography at the University of British Columbia. The availability of digital data from this station has greatly increased the number of useful images being archived.

East Coast Imagery

As mentioned earlier a limited number of both summer and winter/spring images were available for the east coast. The primary region of main interest was selected as the Labrador coast between Cape Chidley and Hamilton Inlet along with the mouth of Hudson Strait and all of Ungava Bay. Off the Labrador coast the cold Labrador Current flows south carrying water from Davis Strait down to the coast of Newfoundland. Some of this water enters into Hudson Strait at the north while other water discharges from the Strait eastward to join the Labrador Current. These general flow patterns are clearly depicted in the 0/1000 db dynamic height contours drawn by Smith (1937) and presented here as Fig. 1. This mean flow pattern also shows how the discharge at the mouth of Hudson Strait separates into both offshore and nearshore portions leaving part of the area just south of Cape Chidley without a strong mean flow. This will be seen in the infrared imagery as a region of complex temperature patterns representative of the small scale structure in this area between the two branches of the Labrador Current. As can also be seen in Fig. 1 these two current branches reunite just north of Hamilton Inlet where the current turns eastward along the geographic boundary. The union of these two current branches is also revealed by the satellite images which show cold coastal waters joining with the cold offshore portion of the Labrador Current. These patterns are also apparent in winter when the ice appears to frequently display a clear region in the region just southeast of Cape Chidley. Similarly the ice patterns appear to change just north of Hamilton Inlet with the wavelike features observed by LeBlond (1982) increasing in amplitude at this point.

Returning to summer images the most striking characteristic of the image in Fig. 2a is the close correspondence between the position and shape of the interface between the cold and warm surface waters and the shape and location of the continental slope. In Fig. 2b this surface temperature boundary has been drawn schematically on a map of the coast which also shows the bottom topography. The similarity between the 2000 m contour and the surface temperature front suggests the topographic steering of the current associated with the temperature gradient. Of particular interest is the sharp seaward meander of the boundary over the small topographic ridge slightly northeast of Hamilton Inlet. This same image (Fig. 2a) also demonstrates how the current turns away from the coast at about 55°N as the current narrows to round the coast leaving a large patch of warm surface water nearest the coast off Hamilton Inlet. The outer boundary of the cold water also turns seaward following the path of the 2000 m contour. Relatively small patches of cold water farther offshore suggest that meanders of the cold current band may separate to form eddies. While these eddies appear cold at the surface their sense of rotation must be anti-cyclonic if formed as meanders of the southbound current. This and other images suggest by the shape of the features that they may be rotating clockwise consistent with this formation mechanism.

In Fig. 3a, another summer image collected on August 19, 1980, the outer boundary of the cold tongue again follows the continental slope lying between the 1500 and 2000 m depth contours. Unlike the image from July 1979 the cold core of the Labrador Current is quite narrow and highly meandered. The patch of warm water off Hopedale, north of Hamilton Inlet, is broken by tongues of cold water extending shoreward in from the cold core of the Labrador Current.

Just southwest of 57°N, 58°W a sharp "v" shaped meander marks a shoreward meander of the current. Oddly enough another image just one year earlier also exhibited a "v" shaped meander at about the same location. It is possible that the small topographic ridge at this position (Fig. 3b) is responsible for the quasi-permanence of this meander feature.

An interesting series of images from the summer of 1981 covers the region of Ungava Bay, the mouth of Hudson Strait and the northeast coast of Labrador. In an image from June 28 (Fig. 4), there is a concentration of warm water along the eastern boundary of Ungava Bay which extends northward in a 30 km band. This warm band narrows as it turns east to round Cape Chidley extending out to almost 62°W. From this image alone it is not clear if this warm water joints with that just to the southwest which separates the cold cores of the in and offshore branches of the Labrador Current.

It is interesting that just north of this warm water exiting Hudson Strait is a narrow band of cold water which also appears to originate within the Strait. This cold band is then separated from the cold waters which ring Resolution Island by warm water which seems to turn into the mouth of Hudson Strait from farther north. East of 63°W this warm water turns to cold which appears to be flowing south to connect with the offshore branch of the Labrador Current.

About three weeks later a cloud-free image from July 15 (Fig. 5) reveals a somewhat different pattern. As on June 28 there is warm water in a band along the eastern boundary of Ungava Bay; at this later time the band reveals eddy-like patches in the south an a branch extending westward from 60°N, 66°W. This coastal warm band is again about 30 km wide but no longer extends eastward around the northern tip of Labrador. Instead cold water flows out of the central mouth of Hudson Strait to then split into a narrow coastal branch and a wider offshore branch of the Labrador Current. The warm water between these branches is highly meandered and eddied with filaments of warm and cold water marking both cyclonic and anticyclonic rotations. The nearshore portion of the coastal branch also appears meandered with small patches of warm water.

Finally on July 29 (Fig. 6) this pattern has been amplified with cold water coming out of Hudson Strait and clearly splitting just southeast of Cape Chidley into near and offshore cold bands representative of the branches of the Labrador Current. The warm water between these branches is similar in shape and location to its expression in the image two weeks earlier (Fig. 5). Again interesting is the warm tongue just north of 61°N which turns westward into the mouth of Hudson Strait. This warm tongue, and its connection to the warm water along 64°W, are seen in all three images. This separation strongly suggests that the coastal branch, of the Labrador Current, is fed by the discharge from Hudson Strait rather than from water flow south out of Davis Strait.

A late spring image from May 29, 1981 (Fig. 7) contains an open area southeast of Cape Chidley where the warm water was seen in summer. In this image the open water area is quite large and stretches south to about 59°N. Southward the ice is fairly broken up and fragmented with large open leads adjacent to the coast. Ungava Bay appears ice covered and some ice can be seen extending out through the mouth of Hudson Strait. The outer edge of this ice cover is just inside and roughly parallel to the 500 m bathymetric contour. Ice patterns similar to those discussed by LeBlond (1982) were observed as shown for example in Fig. 8, a visible image from April 18, 1982. In this image the area just southeast of Cape Chidley is once again clear of ice and a number of other open leads appear nearshore farther down the coast. The seaward edge of the pack ice is composed of offshore extending tongues of many different length scales. Some appear associated with definite cyclonic features while others are likely expressions of anticyclonic eddies. The most prominent feature is a warm patch with a cold center between 59 and 59°N along 61°W. This and many other features have size scales around 50-60 km similar to the 73 km wavelength inferred from visible satellite images by LeBlond (1982). Also consistent with LeBlond's study are the southeastward extending tongues of ice off Hopedale at the lower right of the image. As with the four visible images analyzed by LeBlond (1982) these tongues appear to grow in amplitude toward the south.

In summary both summer and winter images from the Canadian east coast have demonstrated the close correspondence between sea surface temperature expressions of the Labrador Current and the shape of the continental slope. The outer edge of the cold band marking the

Labrador Current appears to follow the outer portion of the slope running along the 2000 m depth contour. Smaller scale changes in the shape of the continental slope lead to meanders and eddy formation in the Current. In winter coastal pack ice cover also exhibits wavelike meanders which grow in amplitude towards the south. Just southeast of Cape Chidley the cold Labrador Current waters splits into coastal and offshore branches. Cold water discharged from Hudson Strait contributes to both of these current branches. The area between these two branches is usually warm in summer and ice free in winter/spring.

West Coast Imagery-Baroclinic Instability

Our study of infrared satellite imagery off the Canadian west coast has focused on the region off Vancouver Island and the northern part of Washington State as shown in Fig. 9. Earlier studies of this region (Mysak, 1977; Emery and Mysak, 1980) suggested that tongue-like meanders in the infrared sea surface temperature exhibited length scales and growth rates consistent with their formation through the mechanism of baroclinic instability. As first modelled by Mysak (1977) this instability transferred energy from the shear between a northwestward undercurrent flow, and a deeper layer at rest into these meanders. Later Wright (1980) added a third layer to this model and concluded that the energy transfer was from the shear between the southeastward surface current and the underlying northwestward undercurrent to the meanders. The presence of this undercurrent, called the California Undercurrent, as far north as Vancouver Island has been discussed by Hickey (1979).

All of these earlier studies looked at a very limited number of satellite images and thus relied primarily on analytical models to reveal characteristics of the instability mechanism and the associated flow system. In the present study we have used a large number of relatively cloud-free images from the period between 1980 and 1982. We have also been fortunate in having current meter data available for 1980 collected off the west coast of Vancouver Island by scientists at the Institute of Ocean Sciences at Patricia Bay, B.C. Temperature and salinity data, collected in conjunction with these current meter data, have also served to independently confirm our conclusions based on the satellite imagery and numerical modelling.

The best series of surface temperature images is from the summer of 1980. Starting on July 21 (Fig. 10) the image reveals a warm sea surface off the coast of Vancouver Island. The only exception in this image is a patch of cold water off the mouth of the Strait of Juan de Fuca. As discussed by Freeland and Denman (1983) this is the expression of a cold cyclonic eddy driven by the interaction between the undercurrent and the topographic irregularity of the Juan de Fuca Canyon (Fig. 9). In summer this cold patch is almost always present independent of whether or not wind-driven upwelling is occurring. In response to southeastward alongshore wind coastal upwelling produces a band of cold water off the coast of Vancouver Island (Fig. 11, July 28) which appears highly meandered with a relatively short spatial scale. Cold water can also be seen along the coast of Washington and in the Strait of Juan de Fuca. On August 24 (Fig. 12) these meanders have developed into a series of six tongues spaced about 75 km apart. A sequence of six images documents the evolution of the surface temperature field between this August 25 image and Fig. 13 the image from September 14. Here only three tongues are apparent with a spacing of about 150 km. The largest of these is shaped somewhat like a "T" and is the expression of a pair of matched, counter-rotating eddies we called "dipole eddies". On October 2 (Fig. 14) the image records the separation of these tongues into a series of three distinct cold cyclonic eddies with the central feature being much larger than the eddies to the north and south. This pattern of surface temperature evolution is summarized in Fig. 15 where the reference line represents the position of the continental shelf break. Fourier spectral analyses of these images confirms the shift from both 75 and 150 km features in July and August to only 150 km features in September and October.

Linear instability theory, for the summer current conditions of a southward surface flow over a northward undercurrent, yields a fastest growing wavelength of about 100 km. This is between the 75 and 150 km wavelengths observed in the imagery from the summer of 1980. As a possible solution to this discrepancy non-linear numerical calculations were carried out for the summer conditions. The model used had four layers in the vertical and represented the flow seaward of the continental shelf-break as shown graphically in Fig. 16. Also shown here is the vertical mean current profile used in the model. This model was initiated with small amplitude 75 and 150 km scale meanders. As represented schematically in Fig. 17 the evolution of this model over a 44 day period demonstrates the early growth of the shorter scale meanders which then weaken to transition into the larger 150 km meanders which then form into discrete cold cyclonic eddies. During this evolution the formation of dipole eddies is evidenced about 30 days into the model run. Thus the non-linear numerical model correctly simulates the events inferred from the infrared satellite images and explains why the linear theory fails to predict the proper meander wavelength. This is quite reasonable since in the summer the very strong shear between the southward surface current and the northward undercurrent would lead to the increased influence of non-linear energy transfer mechanisms. An energy analysis of the numerical results reveals that while both barotropic and baroclinic instability mechanisms are operating the baroclinic instability accounts for more than 80% of the energy transfer. Looking at *in situ* oceanographic data from 1980 Thomson (1984) also concludes that baroclinic instability is primarily responsible for the formation of cyclonic eddy seen just off Vancouver Island in the same location as the northernmost meander and later eddy in Figs. 12 and 13.

In searching for an initial generating mechanism, for the smaller scale 75 km meanders, it was observed (Ikeda, et al., 1984a) that the continental slope off Vancouver Island contains variations with an alongshore scale of about 75 km (Fig. 9). To evaluate the possible role of these bottom topography variations another numerical simulation was run with no initial meanders but a bottom topography with topographic bumps that extended into the second or undercurrent layer (Fig. 18). Run over a time similar to that for the earlier model this simulation demonstrated the excitation of the

75 km meanders by the interaction of the undercurrent with the irregularities in the bottom. These short scale meanders grew initially and then transferred energy via a non-linear interaction into the large 150 km scale features which then shed independent cold eddies (Ikeda, et al., 1984b). Thus the summer evolution is a "red-cascade" from small scale 75 km meanders, started by an interaction with the bottom topography, to longer 150 km meanders which then shed cold cyclonic eddies in a period of a month to six weeks. This sequence of surface temperature features has also been observed in the infrared satellite imagery from the summer of 1982 (Ikeda, et al., 1984b).

In winter and spring the mean current (0-1000 m) off Vancouver Island is all directed northwest or southeast respectively. The absence of the undercurrent during these periods is discussed by Hickey (1979) and is clearly represented in the current meter records from the west coast discussed by Freeland, et al. (1984). Late fall and winter satellite images appear to contain only larger scale meander features with wavelengths of about 120 to 150 km, as shown for example in Fig. 19, an image from November 27, 1981. Interestingly linear instability theory predicts wavelengths of this magnitude for winter flow conditions.

In spring the uniformly flowing southward current also leads to longer scale features as predicted by the linear stability theory. Imagery from this season again exhibit larger scale features between 120 to 150 km consistent with the scales of linear theory. A sample spring image is shown in Fig. 20 for April 6, 1982. Here as in other images the cold/warm boundary has been outlined to better define the meanders revealed by the surface temperature patterns. It should be noted that while in summer the boundary is between cold, upwelled coastal water and warmer water offshore, in spring the boundary marks meanders as seaward extending tongues of warm water off of Vancouver Island. While this appears to contradict the geostrophic relationship it should be remembered that especially in spring salinity plays a significant role in establishing the coastal current (Tabata, 1976).

That this instability mechanism may be operating farther south along the west coast of North America is suggested by the marked tongue-like meanders in Fig. 21, a satellite image from the area off northern California and Oregon collected on September 13, 1982. Fourier analysis of this and other similar images suggests that again 150 km meanders dominate later in the summer. In these images, however, there is also a 200 km length scale which appears to be associated with the large horizontal scale of the topographic ridges in this region. Thus once again both bottom topography and non-linear interaction appear to influence the formation of current meanders as expressed in infrared satellite sea surface temperatures. As recently discussed by Mooers and Robinson (1984) meanders, eddies and even dipole eddies have been observed in hydrographic data collected in this region during summer. This provides independent evidence of the instability mechanism inferred from the infrared satellite imagery.

In summary surface temperature patterns, as revealed by infrared satellite imagery, contain large scale (120-150 km) meanders in spring and winter consistent with the length scales predicted by linear instability theory for these seasons. In summer non-linear mechanisms are more important and a non-linear numerical model simulates the evolution of meanders from an initial scale of about 75 km to that of 150 km over a period of about 45 days as seen in series of summer infrared satellite images. In summer the meanders appear as cold tongues of upwelled water extending seaward from the continental shelf. Numerical simulation also documents the excitation of the initial 75 km meanders by similar sized variations in the bottom topography. In all cases the primary instability mechanism is a baroclinic transfer of energy from the mean shear into the meanders. In summer the large-scale meanders grow to eventually shed cold cyclonic eddies thus dissipating energy from the mean flow. Satellite images from northern California and Oregon also appear to exhibit surface temperature patterns consistent with this baroclinic instability mechanism.

CONCLUSION

Satellite infrared images from the Canadian east coast suggest a relationship between the path of the Labrador Current and the shape of the continental shelf break. Water from Hudson Strait is seen to contribute to both the near and offshore branches of the Labrador Current which is seen to separate just southeast of Cape Chidley. Between the current branches the ocean is relatively warm in summer and generally ice free in winter/spring. Also related to the shape of the continental shelf break, current meanders form off the Canadian west coast and appear as tongues of warm and cold water in infrared satellite images. Length scales of these meanders (120-150 km) are consistent with linear instability theory in spring and winter while non-linear numerical simulations correctly reproduce the summer/fall meander evolution from 75 to 150 km length scales. Baroclinic instability associated with the structure of the mean flow is responsible for the growth of these meanders and the subsequent shedding of cold, cyclonic eddies.

ACKNOWLEDGEMENTS

This research was supported by the Canadian Natural Sciences and Engineering Research Council, under their Strategic Grants Program for Oceans; this support is gratefully acknowledged.

REFERENCES

Emery, W.J. and L.A. Mysak, 1980: Dynamical interpretation of satellite sensed thermal features off Vancouver Island. J. Phys. Oceangr., 10, 961-970.

Freeland, H.J. and K.L. Denman, 1982: A topographically controlled upwelling centre off southern Vancouver Island. J. Mar. Res., 40, 1069-1093.

Hickey, B.M., 1979: The California Current system - hypothesis and fact. Prog. in Oceanogr., 8, 191-279.

Ikeda, M., L.A. Mysak and W.J. Emery, 1984: Observation and modelling of satellite-sensed meanders and eddies off Vancouver Island, J. Phys. Oceanogr. (in press).

Ikeda, M., W.J. Emery and L.A. Mysak, 1984: Seasonal variability in meanders of the California Current system off Vancouver Island. J. Geophys. Res. (in press).

LeBlond, P.H., 1982: Satellite observations of Labrador Current undulations. Atm. Ocean, 20, 129-142.

Mooers, C.N.K. and A.R. Robinson, 1984: Turbulent jets and eddies in the California Current and inferred cross-shore transports submitted to Science.

Mysak, L.A., 1977: On the stability of the California Undercurrent off Vancouver Island, J. Phys. Oceanogr., 7, 904-917.

Smith, E.H., 1937: The Marion Expedition to Davis Strait and Baffin Bay. U.S. Treasury, U.S. Coast Guard Bull. 19, Part 2, Report of the International Ice Patrol Service in the North Atlantic Ocean, 259 pp.

Tabata, S., 1976: The general circulation of the Pacific Ocean and a brief account of the oceanographic structure of the North Pacific Ocean. Part II - Thermal regime and influence on the climate. Atmosphere, 14, 1-27.

Thomson, R.E., 1984: A cyclonic eddy over the continental margin of Vancouver Island: Evidence for dynamical instability (submitted to J. Phys. Oceanogr.).

List of Figures

16. The four layer model used for linear stability theory and nonlinear numerical simulations.

17. Schematic time series evolution of the surface current axis from the numerical simulation. Numbers in parentheses refer to actual elapsed days.

18. Diagram of topographic obstructive used in the model along with a plan view of the numerical model domain.

19. As in Fig.10 for Nov. 27, 1981.

20. As in Fig.10 for April 6, 1982.

21. Infrared image from the west coasts of Oregon and northern California from Sept. 3, 1982.

ORIGINAL PAGE IS
OF POOR QUALITY

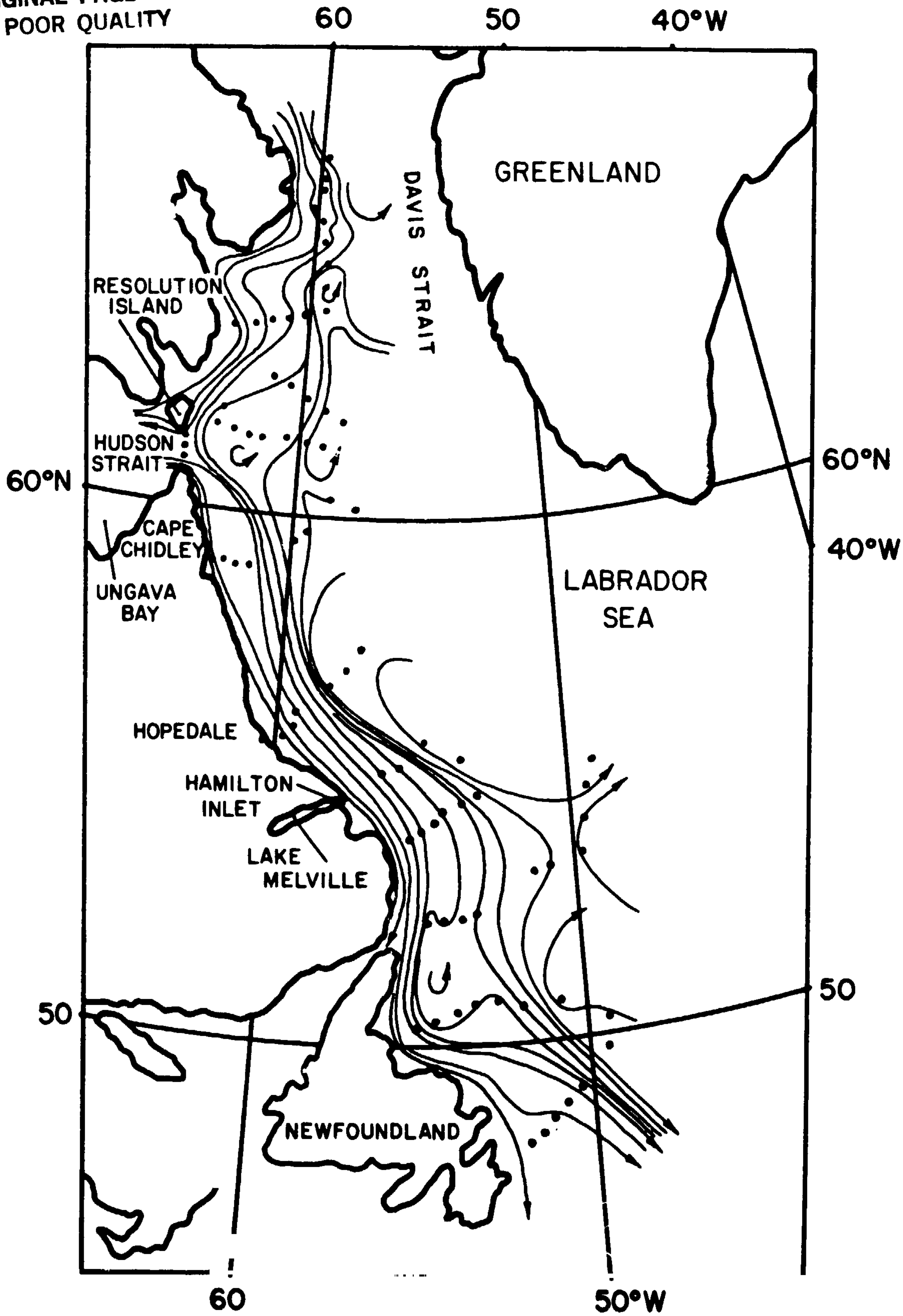

ORIGINAL PAGE IS
OF POOR QUALITY

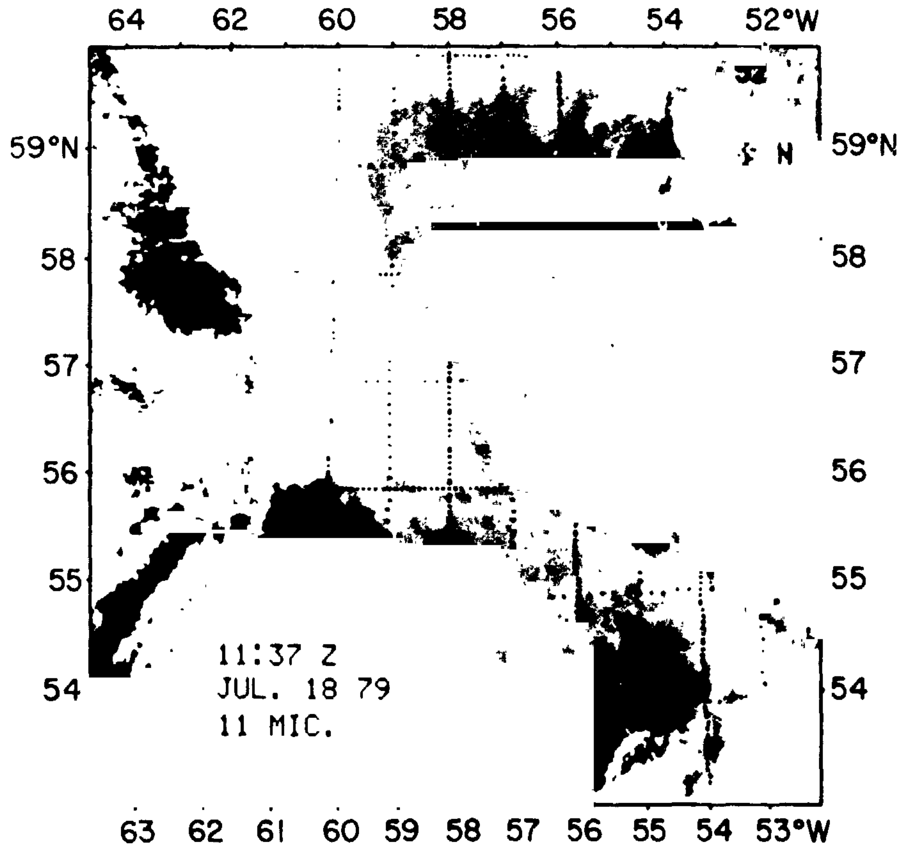

ORIGINAL PAGE IS
OF POOR QUALITY

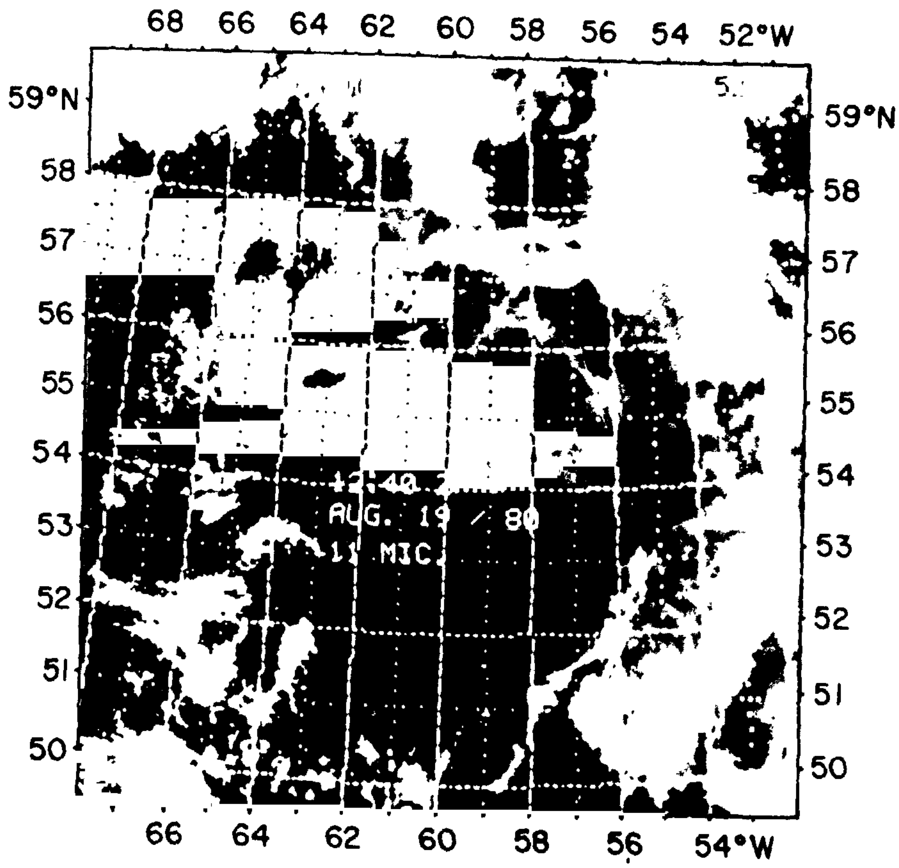

ORIGINAL PAGE IS
OF POOR QUALITY

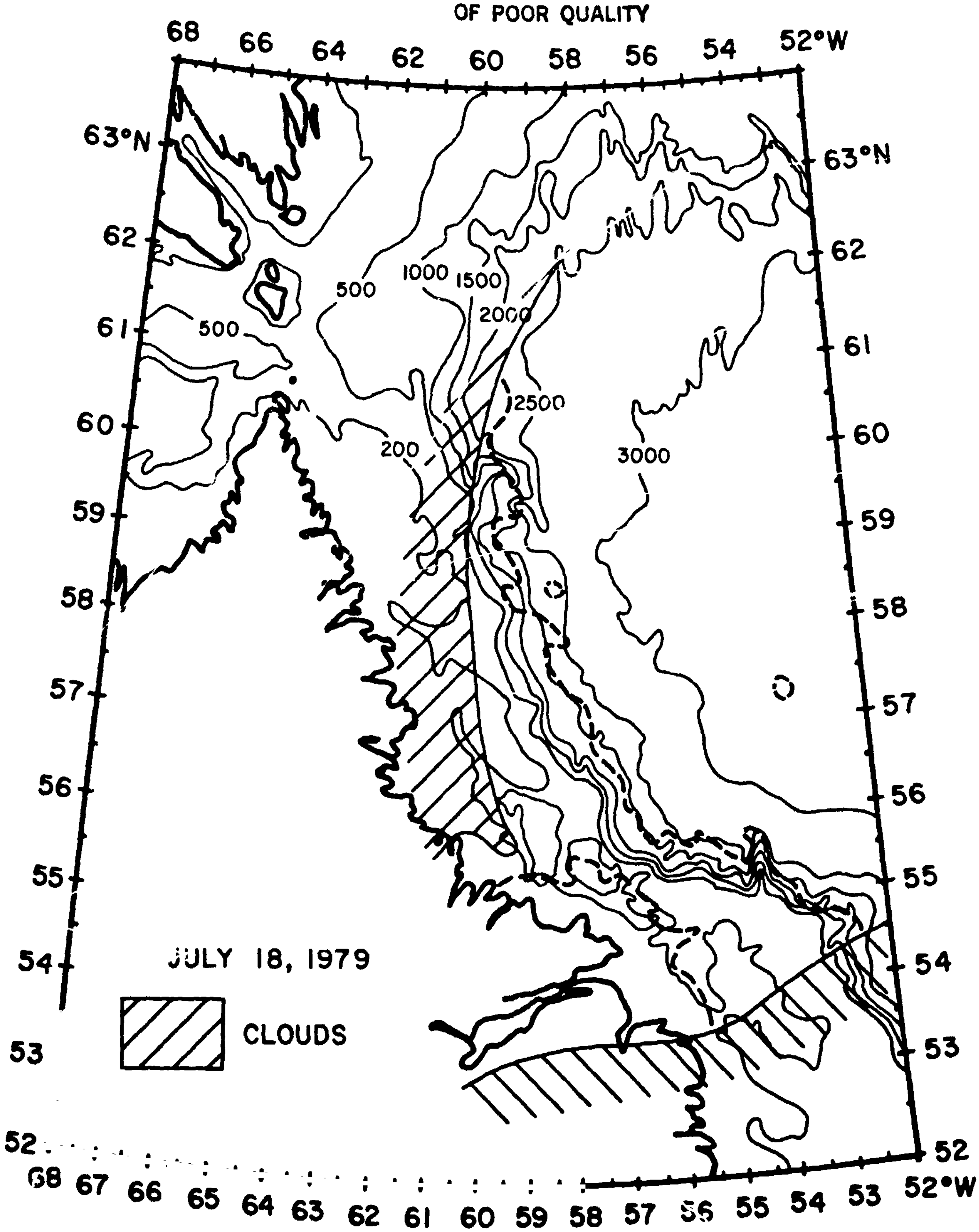

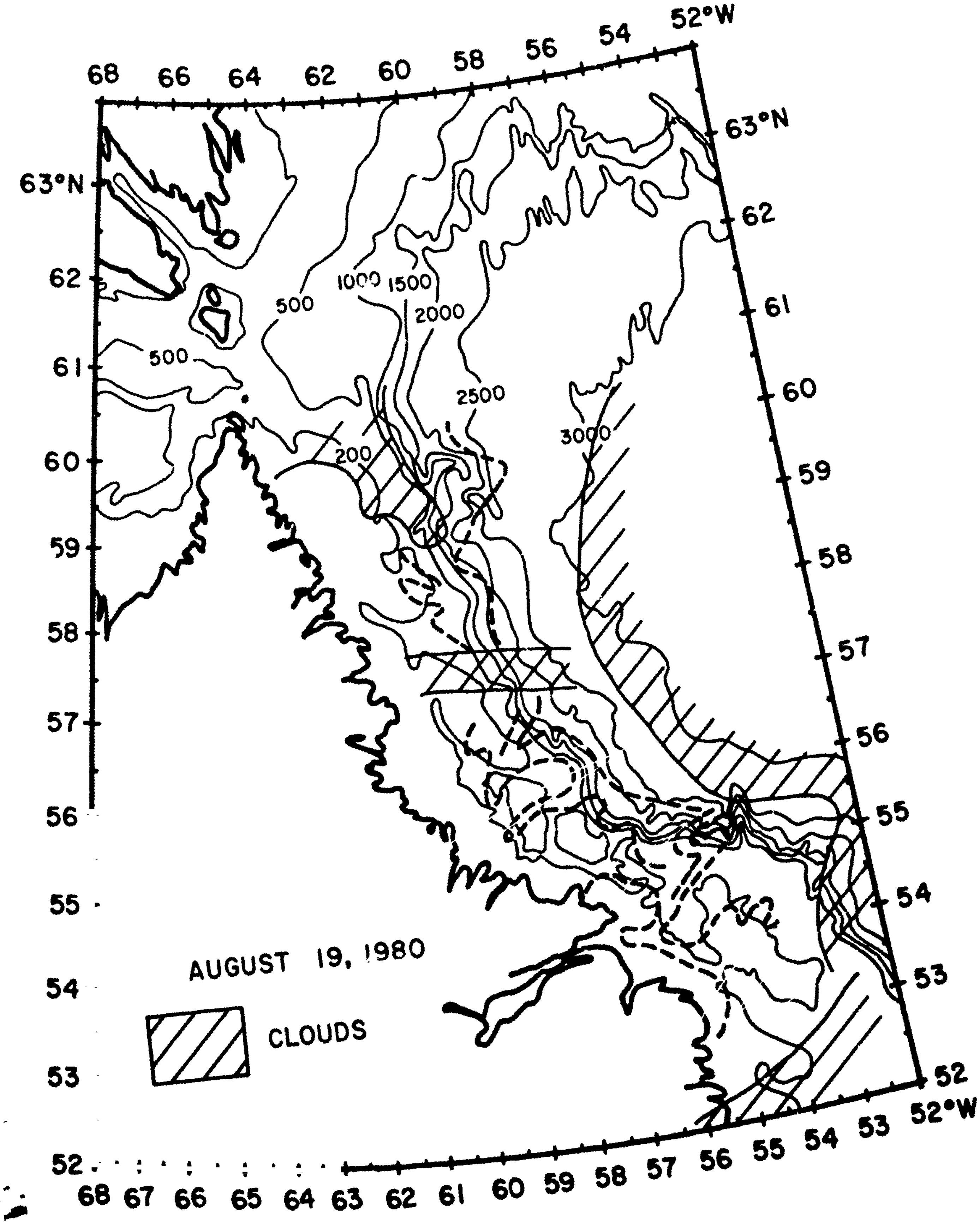
52°W
68
66
64
62
60
58
56
54
63°N
62
61
60
59
58
57
56
55
54
53
52
1000
1500
500
2000
500
2500
3000
200
AUGUST 19, 1980
CLOUDS
68 67 66 65 64 63 62 61 60 59 58 57 56 55 54 53 52°W

ORIGINAL PAGE IS OF POOR QUALITY

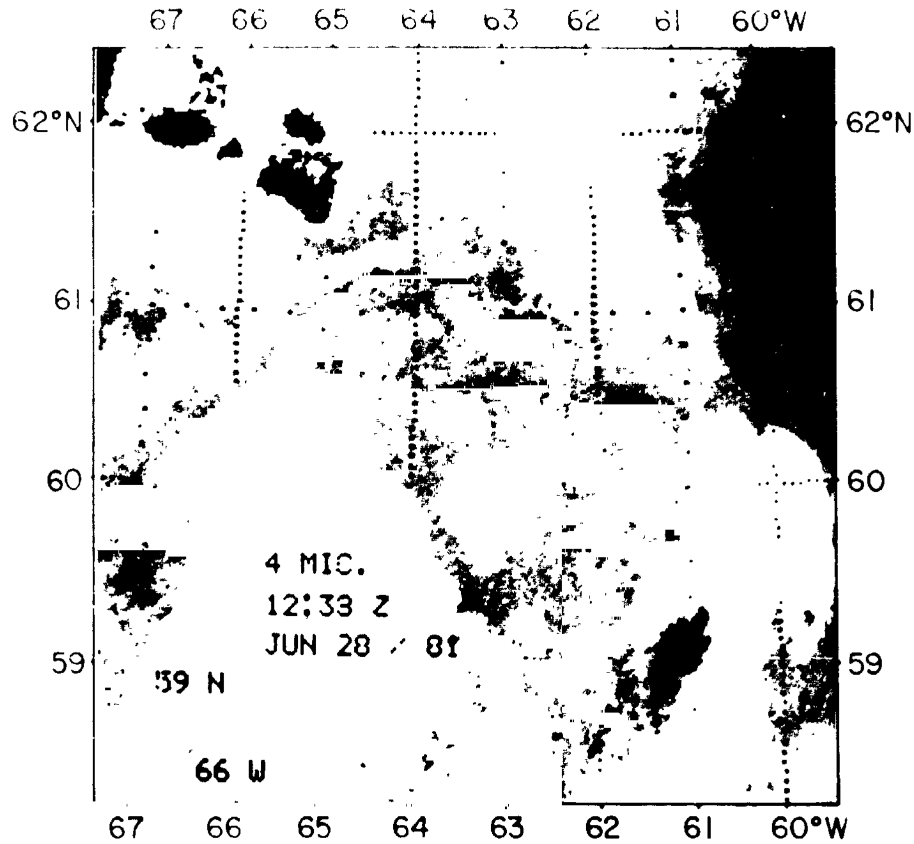

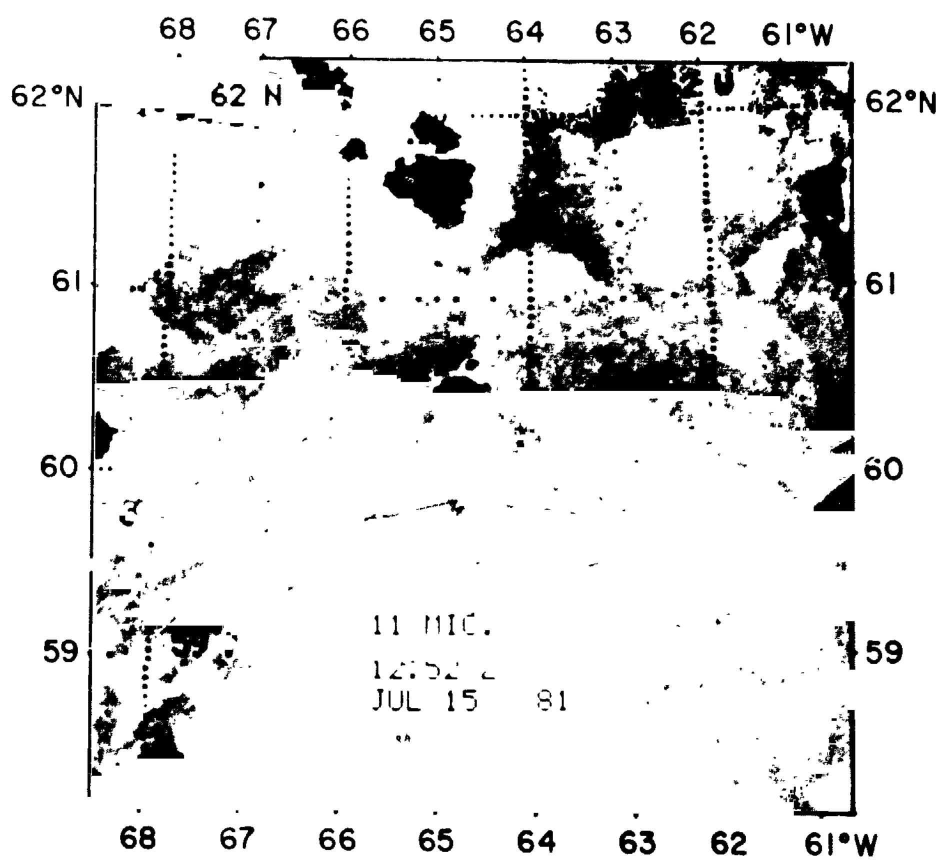

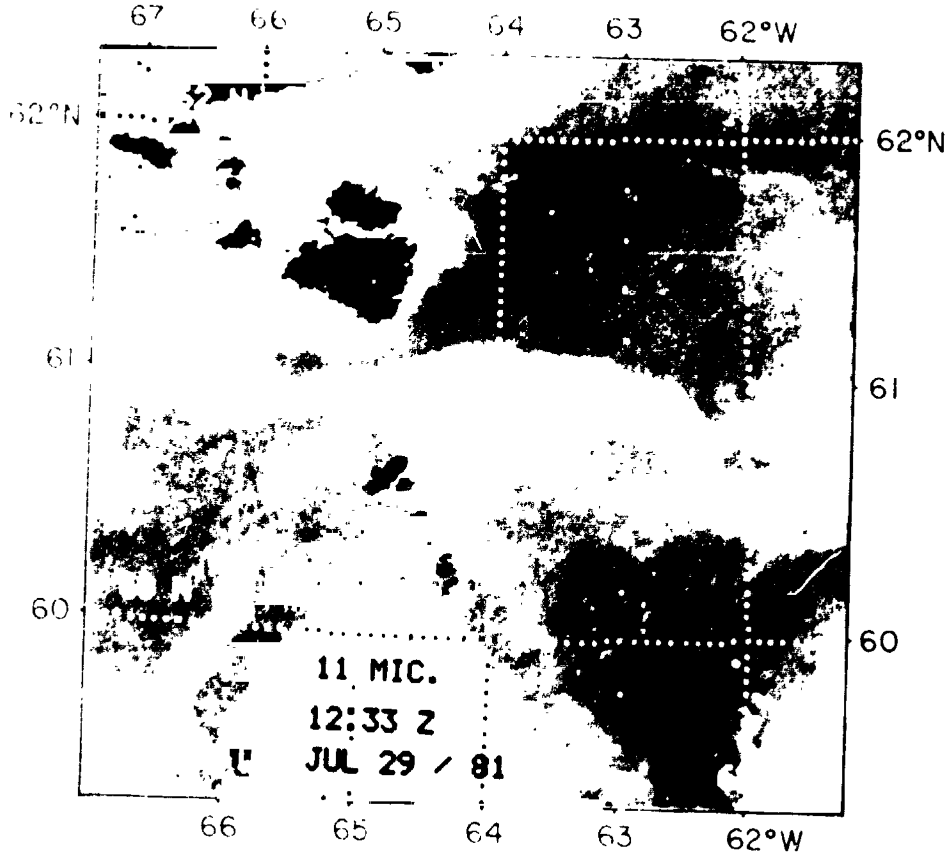
67
66
65
64
63
62°W
62°N
61
60
11 MIC.
12:33 Z
JUL 29 / 81
66
65
64
63
62°W

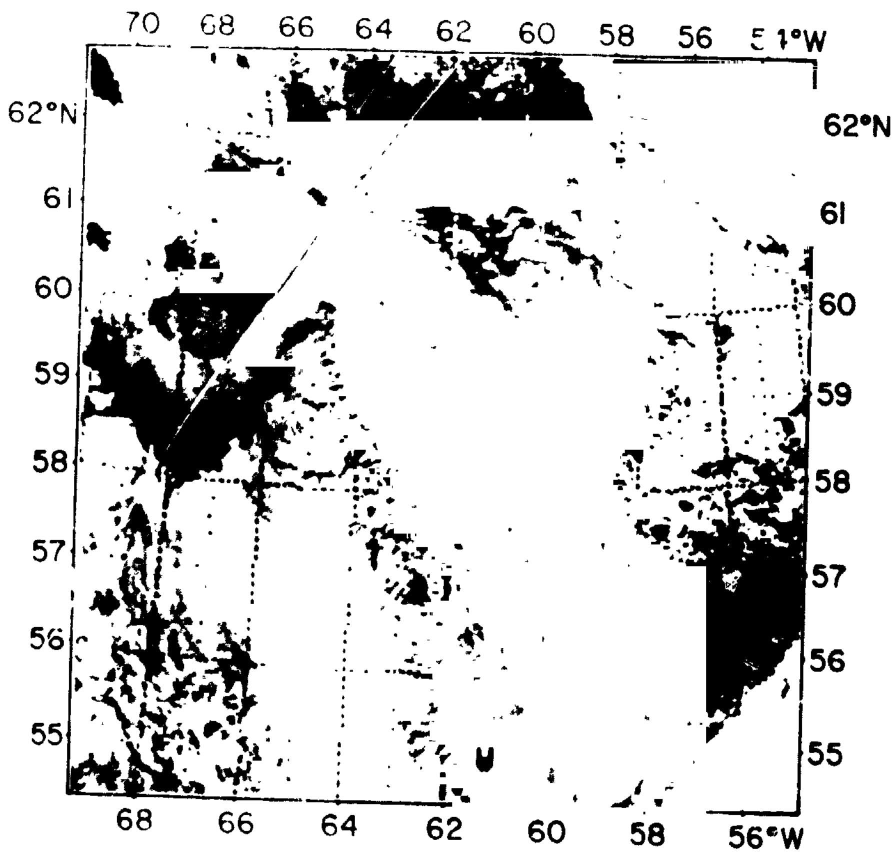
70
68
66
64
62
60
58
56
62°N
61
60
59
58
57
56
55
62°N
61
60
59
58
57
56
55
68
66
64
62
60
58
56°W

ORIGINAL PAGE IS
OF POOR QUALITY

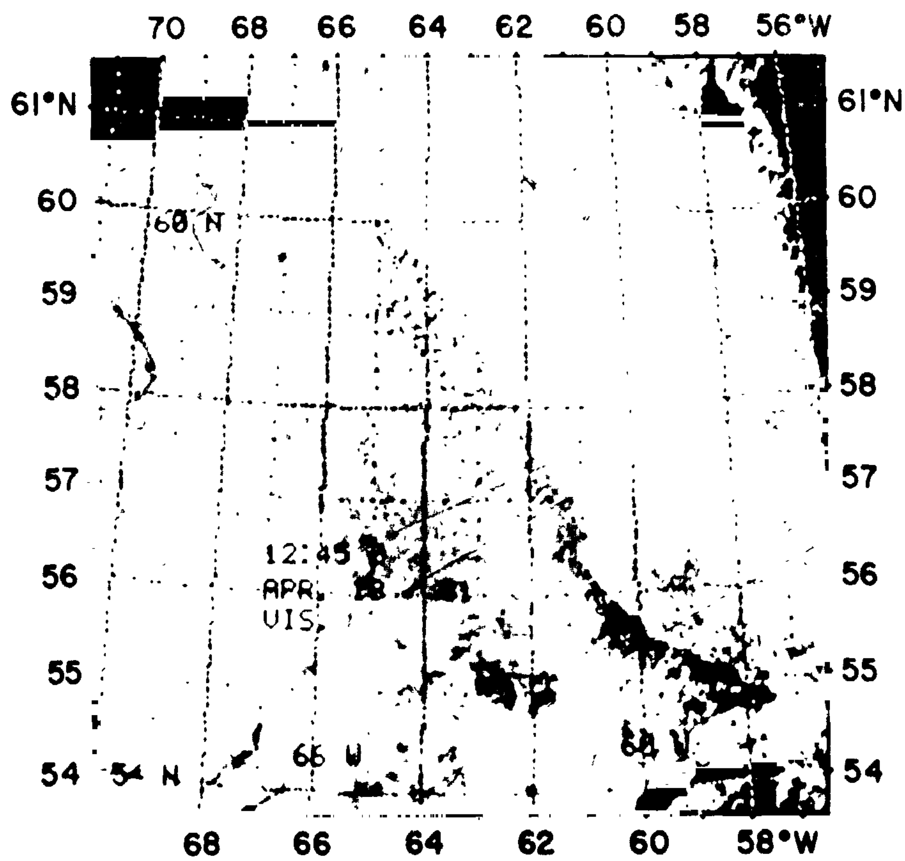

ORIGINAL PAGE IS
OF POOR QUALITY

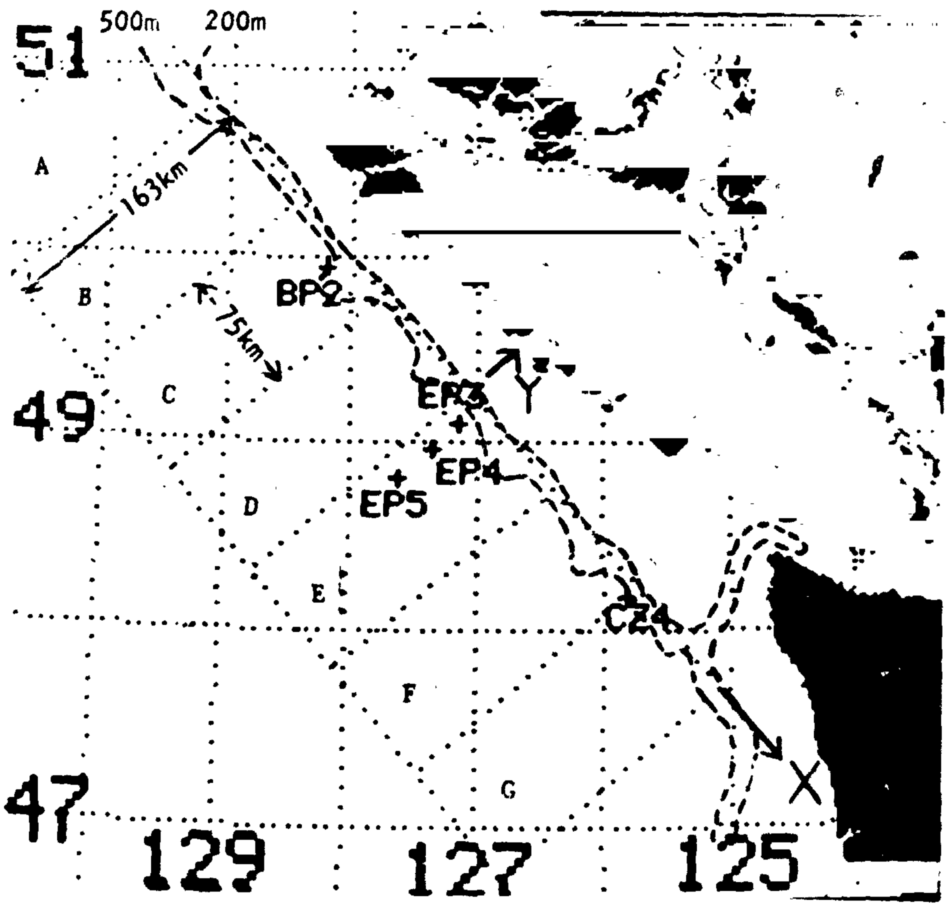

Figure 1 The area observed by satellite infrared images. Nearly vertical and horizontal dotted lines denote longitude and latitude, respectively. Five current meter mooring stations (BP2, EP3, EP4, EP5, CZ4) are indicated by +, 200 m and 500 m-isobaths by broken lines, and the domain of numerical calculations by a long rectangle divided into seven smaller rectangles.

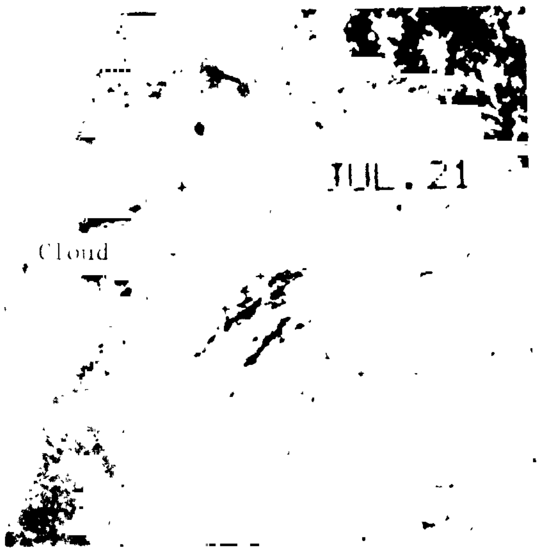
JUL.21
Cloud

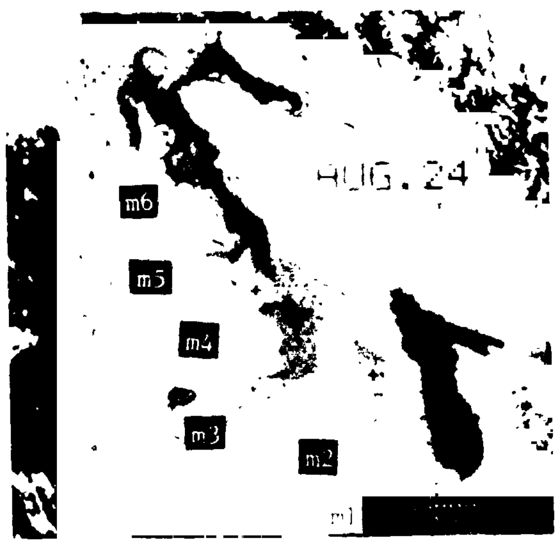
AUG.24
m6
m5
m4
m3
m2
m1


SEP.14

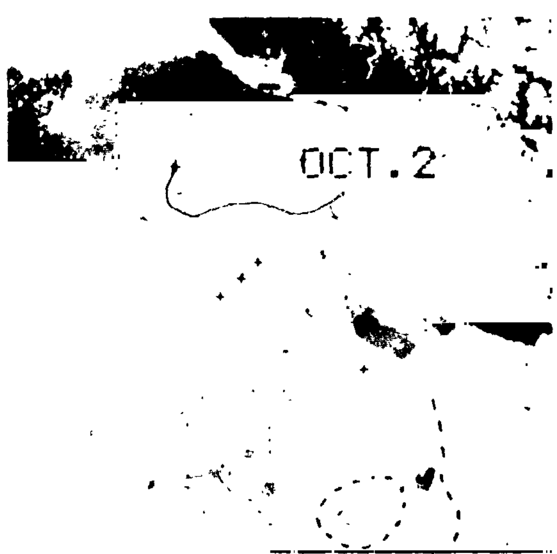
OCT.2

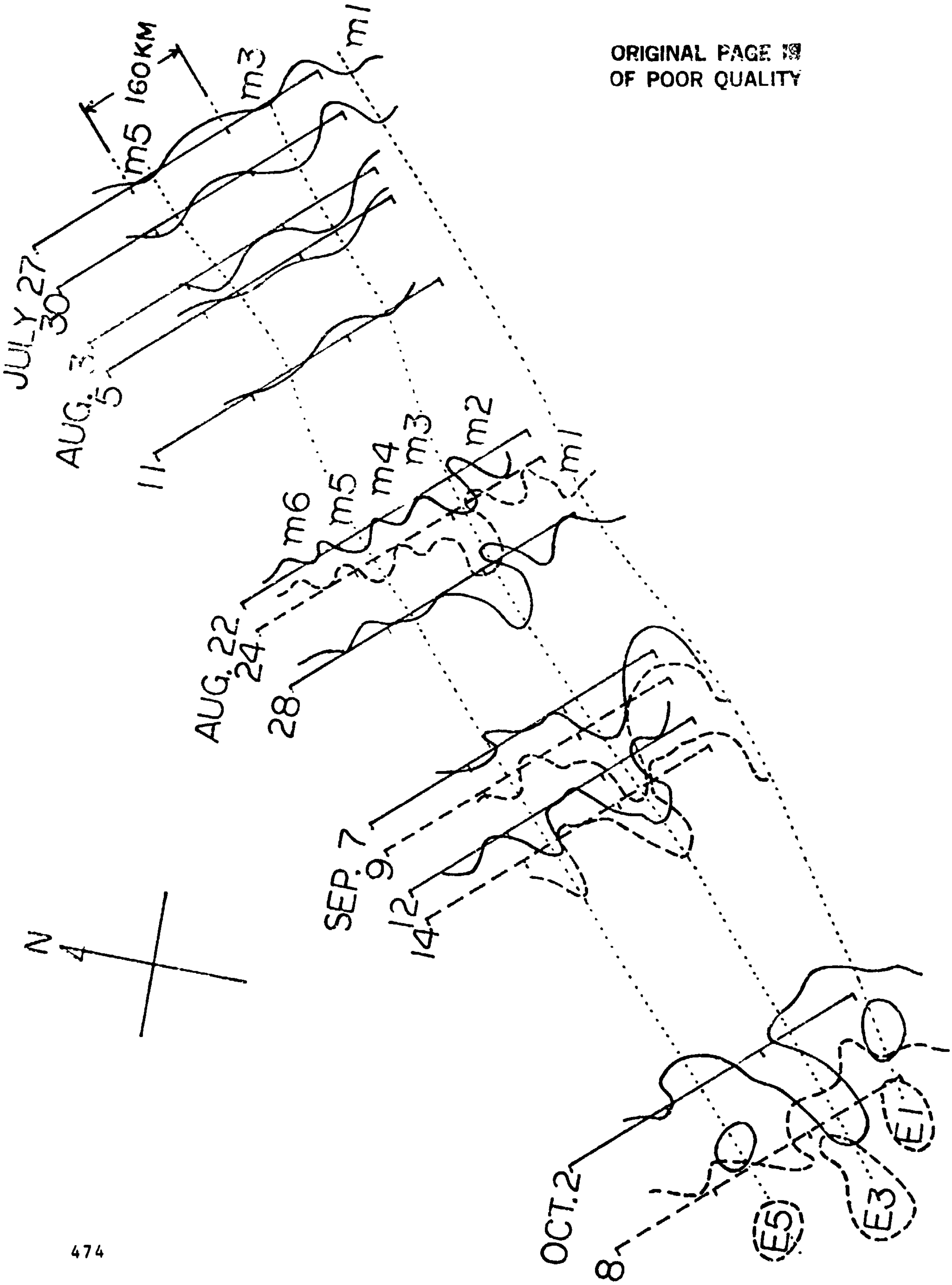
160KM
m5
m3
m1
JULY 27
30
AUG. 3
5
11
m6
m5
m4
m3
m2
m1
AUG. 22
24
28
SEP. 7
9
12
14
N
OCT. 2
8
E5
E3
E1

(a)

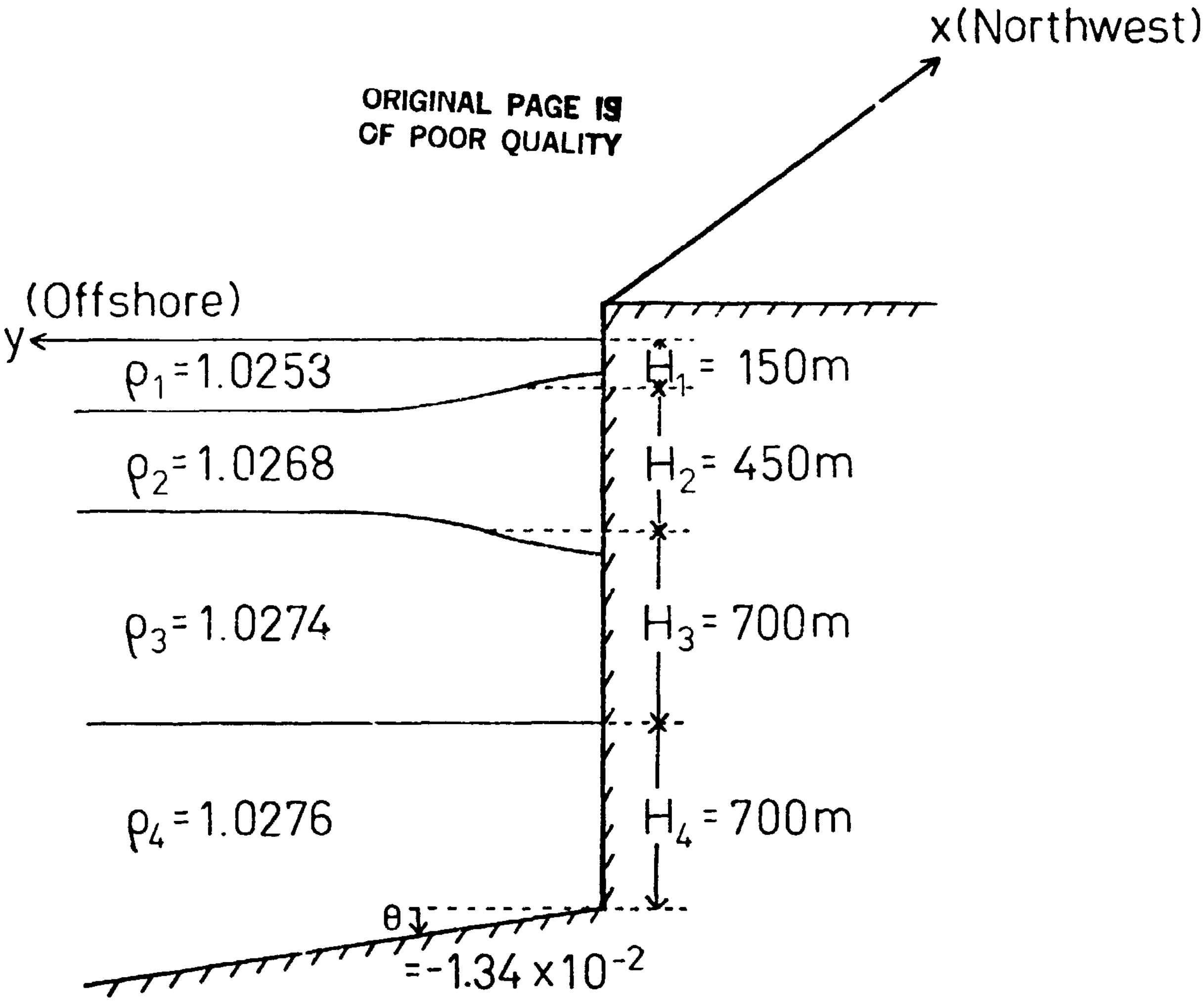
x(Northwest)
(Offshore)
y
ρ1=1.0253
ρ2=1.0268
ρ3=1.0274
ρ4=1.0276
H1= 150m
H2= 450m
H3= 700m
H4= 700m
θ
=-1.34 x 10^-2

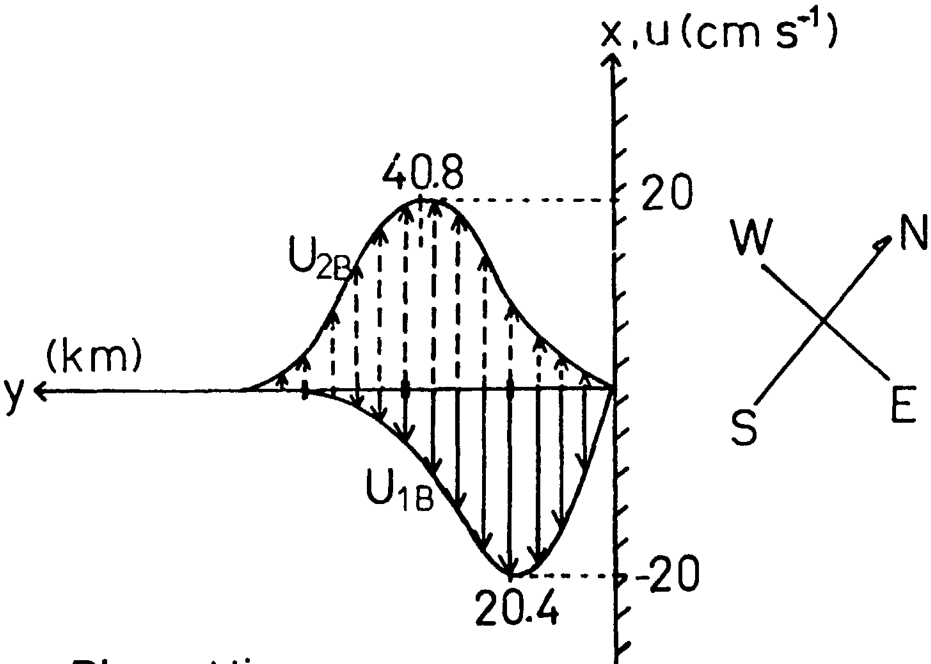
x, u (cm s^-1)
40.8
20
U2B
(km)
y
U1B
20.4
-20
W
N
S
E

Plane View

ORIGINAL PAGE IS
OF POOR QUALITY

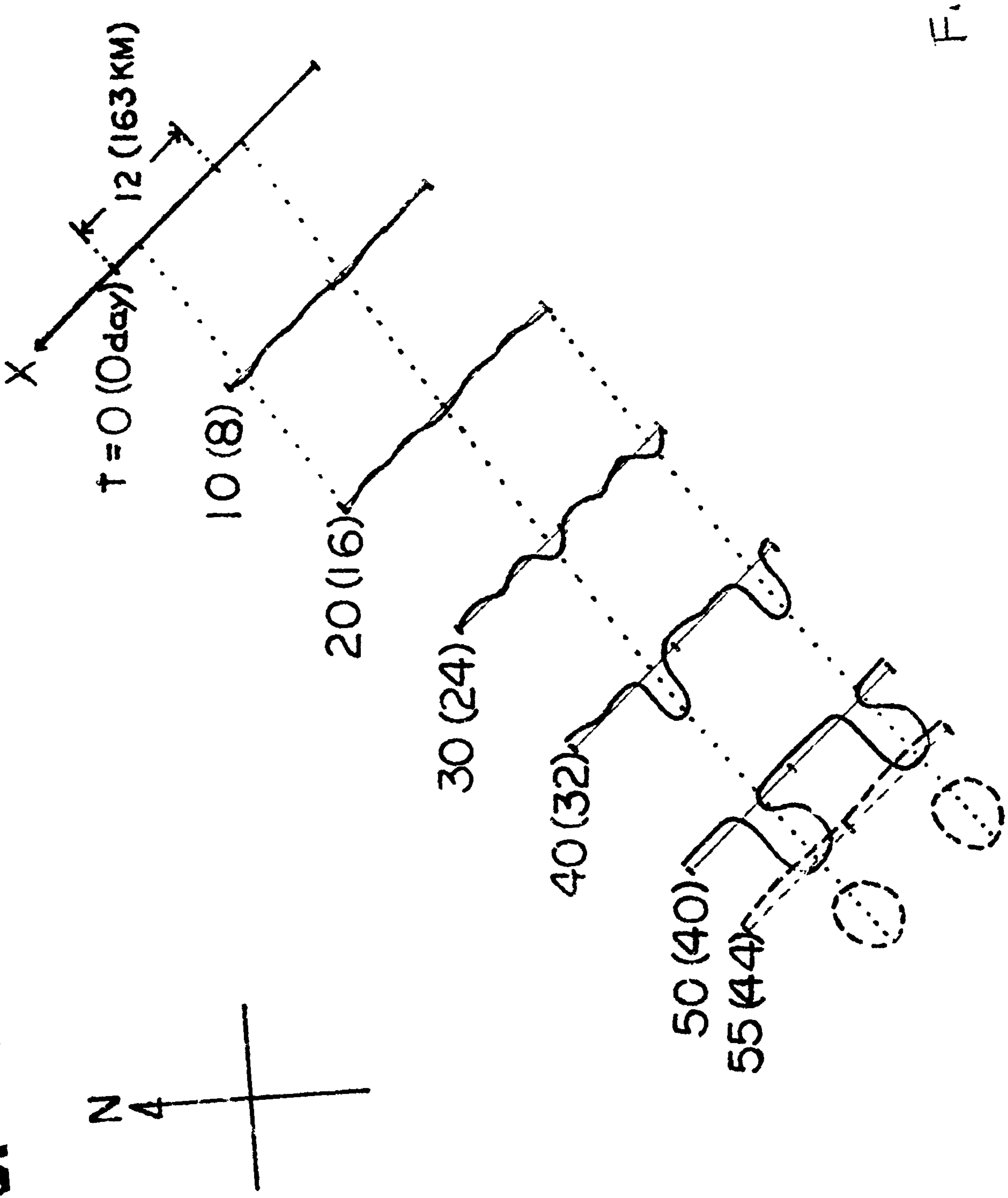

Fig. 17

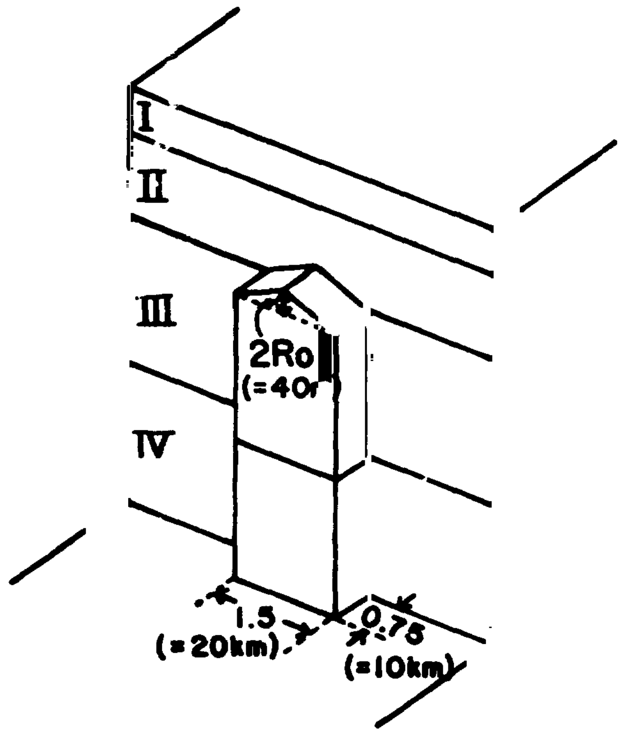

I
II
III
IV
2Ro
(=40r)
1.5
(=20km)
0.75
(=10km)

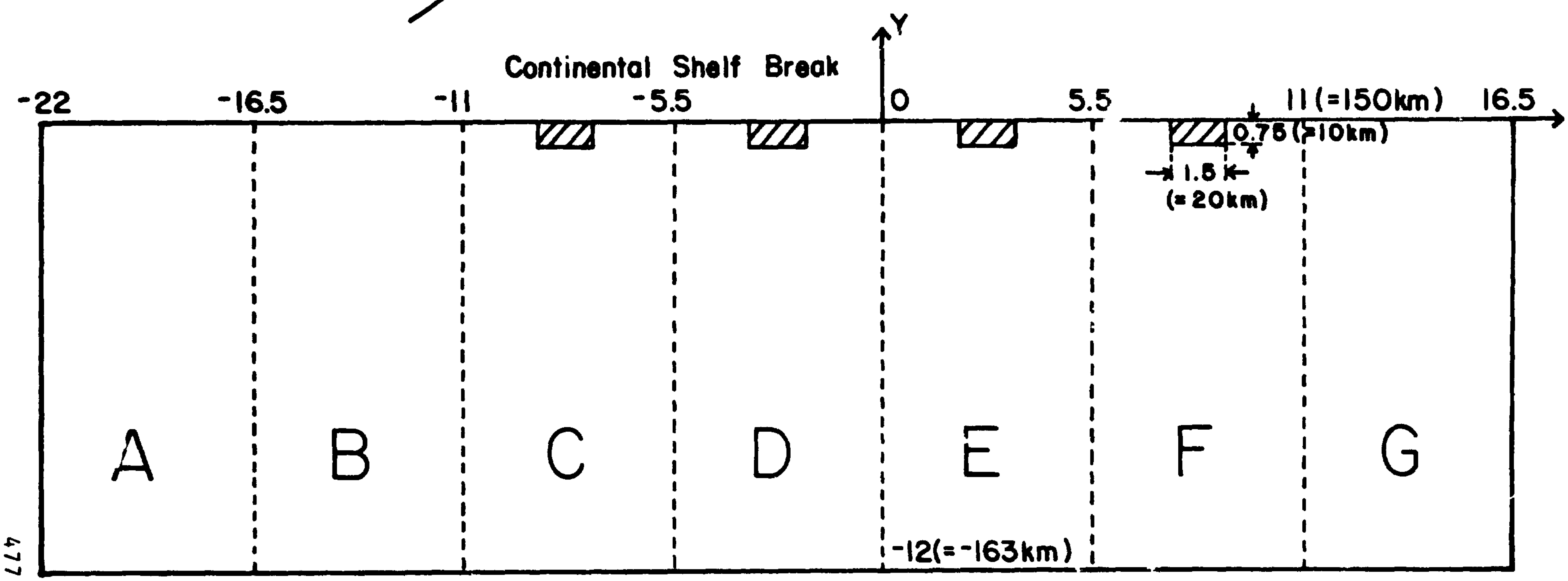

Y
Continental Shelf Break
-22
-16.5
-11
-5.5
0
5.5
11 (=150km)
16.5
0.75 (=10km)
1.5
(=20km)
A
B
C
D
E
F
G
-12(=-163km)

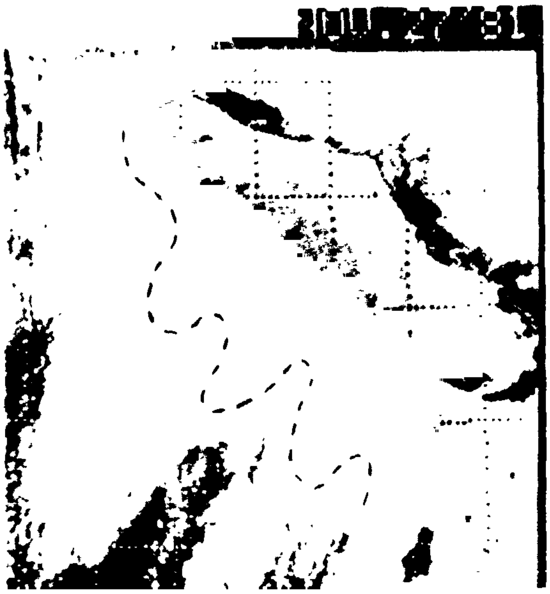

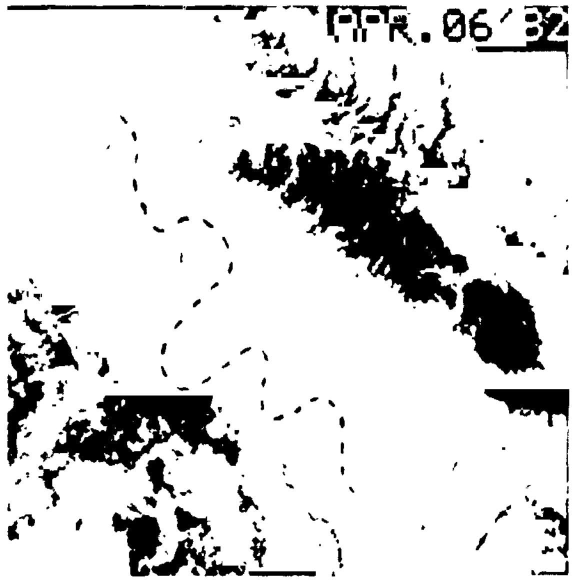

ORIGINAL PAGE IS
OF POOR QUALITY